LUX - A DESIGN STUDY FOR A LINAC/LASER-BASED ULTRAFAST X-RAY SOURCE

J. N. Corlett**, W. A. Barletta, S. DeSantis, L. Doolittle, W. M. Fawley, P. Heimann, S. Leone, S. Lidia, D. Li, G. Penn, A. Ratti, M. Reinsch, R. Schoenlein, J. Staples, G. Stover, S. Virostek, W. Wan, R. Wells, R. Wilcox, A. Wolski, J. Wurtele, and A. Zholents
Lawrence Berkeley National Laboratory, Berkeley, CA, U.S.A.
jncorlett@lbl.gov; phone 510 486 5228; lux.lbl.gov

Abstract

We describe the design concepts for a potential future source of femtosecond x-ray pulses based on synchrotron radiation production in a recirculating electron linac. Using harmonic cascade free-electron lasers (FEL's) and spontaneous emission in short-period, narrow-gap insertion devices, a broad range of photon energies are available with tunability from EUV to hard x-ray regimes. Photon pulse durations are controllable and range from 10 fs to 200 fs, with fluxes 10^7- 10^{12} photons per pulse. Full spatial and temporal coherence is obtained for EUV and soft X-rays. A fiber laser master oscillator and stabilized timing distribution scheme are proposed to synchronize accelerator rf systems and multiple lasers throughout the facility, allowing timing synchronization between sample excitation and X-ray probe of approximately 20-50 fs.

Keywords: ultrafast, x-ray, accelerator, free-electron laser, attosecond, femtosecond

1. SCIENTIFIC MOTIVATION

Ultrafast x-rays have been identified world-wide in numerous workshops and reports as a key area ripe for new scientific investigations [1-6]. Lasers successfully cover most of the visible, infrared, and ultraviolet regions of the spectrum with both high resolution and very short pulses. Thus, experimentalists have utilized lasers to tremendous advantage for thousands of time-dynamics investigations, many critical to the scientific fields of solid-state physics, photochemistry, and photobiology. Until now, ultrafast time domain studies in the x-ray region have been lacking. By use of synchrotron radiation and by novel conversion of intense laser pulses into soft and hard x-rays, scientists have been able to perform some of the first innovative experiments recently, such as Bragg diffraction studies of phase transitions, time-resolved Laue diffraction of myoglobin-CO reversible binding, femtosecond photoelectron spectroscopy, and even attosecond electron redistribution in Auger electron processes [7-10]. However, these laser-based x-ray fluxes are low, the signal levels weak, the synchrotron-based signals have long pulse durations, and experiments are challenging to accomplish by individual scientists. LUX, a ***L***inac/laser-based ***U***trafast ***X***-ray facility concept based on a recirculating linac, provides an increase of x-ray flux by several orders of magnitude, is accessible to a large number of users, with resources available for set-up of pump-probe femtosecond-scale time resolved experiments utilizing ultrafast lasers. Sample damage is kept to a minimum with lower energies and higher repetition rates, in many cases with complete sample regeneration by translation or flow.

While the approximately 40 available light sources in the world are largely limited to static spectroscopies, microscopies, and structures, the LUX concept is designed from the start as a user facility for femtosecond x-ray dynamics, with precise timing as an integral requirement. In the near future x-ray free-electron lasers (FEL's) are expected to demonstrate some of the first exciting ultrafast x-ray studies with an accelerator-based machine [11-13]. The LUX concept is a refined ultrafast x-ray source, offering higher repetition rates but lower pulse energies than the SASE FELs, tunability, and precision timing with other laser sources for excitation and probe experiments. It would accommodate many users simultaneously, while the whole spectrum of already-available x-ray determinations, long a staple at existing synchrotron facilities, and vigorously producing results in all fields of science, would be open to time dependent measurements. The unique design would satisfy an enormous range of pulse properties for each area of specialty.

By combining both diffraction to explore nuclear positions in real time and spectroscopy to interrogate electronic and atomic states and their structural parameters and chemical environments, such a facility represents a powerful combination to address scientific problems. Although pump-probe experiments represent some of the most important techniques, involving a femtosecond laser as a pump and the recirculating linac-based x-ray source as the probe, the facility may also accommodate rapidly emerging multidimensional coherent laser spectroscopies (e.g. three-laser pump beams and an x-ray probe), as well as two x-ray wavelengths, for double-resonance x-ray pump and probe spectroscopies. Novel forms of spectroscopies with x-rays, that have not even been delineated yet, may be possible.

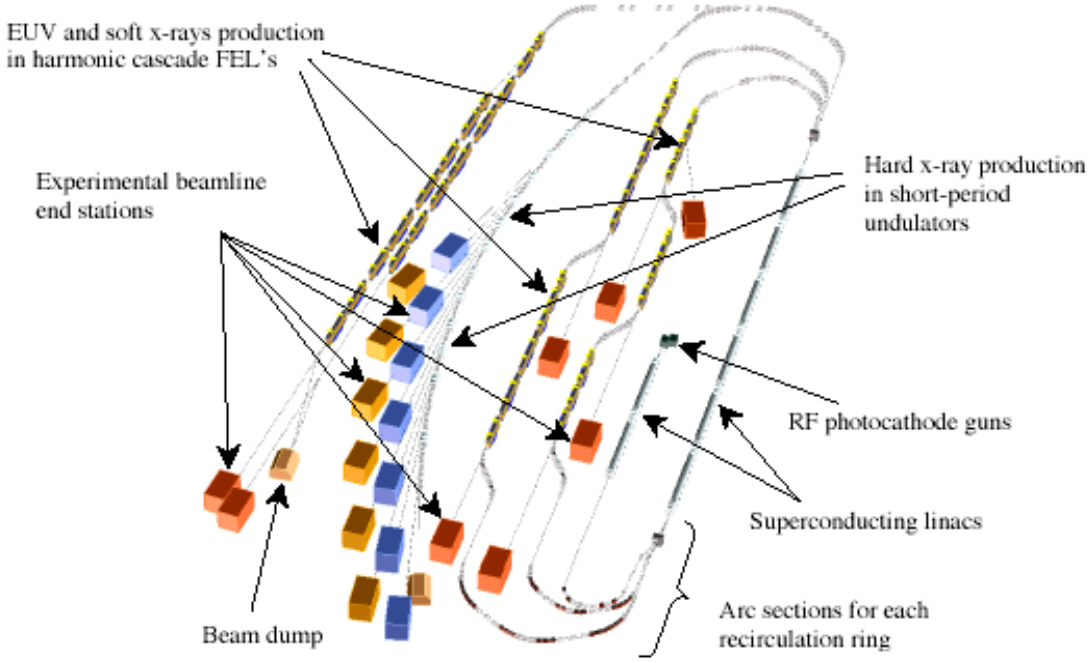

Figure 1. LUX facility concept layout. The machine footprint is approximately 150x50m. A capacity of approximately 20 beamlines is available. The LUX facility concept would provide stable, synchronized, tunable, ultrafast x-ray pulses with variable polarization, and with peak fluxes comparable to third generation light sources, to multiple beamlines operating simultaneously over a broad range of xray wavelengths. An integrated array of lasers at the beamline end stations allows flexibility in sample excitation, synchronized to the x-ray pulse.

In addition to femtosecond-scale pulse durations in LUX, a technique for production of x-ray pulses of approximately 100 attosecond duration has been developed [14]. Access to the sub-femtosecond domain offers great potential of opening a new area of science, studying phenomena on the timescales of electronic transitions [10].

2. ACCELERATOR SYSTEMS

The LUX concept for a ***l***inac/laser-based ***u***ltrafast ***x***-ray facility is based on a recirculating linear accelerator, coupled with an array of advanced tunable femtosecond lasers [15, 16, 17, 18]. The recirculating linac accelerates picosecond duration electron bunches to GeV-level energies. Intense, ultrafast (10's to 100's femtoseconds duration) soft x-rays are produced by cascaded harmonic generation (CHG) scheme [19, 20], similar to high-gain harmonic-generation (HGHG) [21] - a laser-seeded process in a cascaded series of undulators, resulting in enhanced radiation at selected harmonics of the seed. The coherent soft x-rays can be tuned over a range of tens of eV to 1 keV, and ultrashort optical seed laser pulses produce x-ray pulse durations of 10-200 fs. Ultrafast hard x-rays are produced by spontaneous emission of the electrons in narrow-gap, short-period undulators. By use of a novel electron bunch tilting process followed by optical compression, hard x-ray pulse durations of 50-100 fs are obtained over a range of 1-10 keV [22]. Synchronization of the x-rays with lasers is critical for experiments, and optical pulses initiate both CHG seed lasers and experimental end station amplifiers for precise timing [23, 24]. A mode-locked laser provides optical pulses, which are transported around the facility by a stabilized fiber optic distribution system. Radio frequency signals are derived from the master oscillator optical pulse train, allowing phase-locking of remote lasers and all machine rf signals to the master oscillator.

The femtosecond x-rays are produced at a 10 kHz repetition rate, with variable polarization, and with peak fluxes comparable to or significantly greater than existing third generation light sources. The x-ray pulse repetition rate of 10 kHz is matched to studies of dynamical processes (initiated by ultra-short laser pulses) that typically have a long recovery time or are not generally cyclic or reversible and need time to allow relaxation, replacement, or flow of the sample.

The configuration is shown schematically in Figure 1. The major systems are rf photocathode electron sources, an injector linac, a main superconducting linac, arcs to transport the beams of different energies into and out of the main linac, timing and synchronization systems, photon production in a variety of insertion devices, and x-ray beamlines. The basic scheme is as follows, details of key systems are given in following sub-sections: a high-brightness electron bunch is produced in an rf photocathode gun, the beam is accelerated in an injector linac, following which it is transported to the main linac. The beam passes three times through the superconducting

recirculating linac, and on each pass the beam radiates in photon production devices. The beam is finally transported to a shielded beam dump.

The recirculating linac configuration allows flexibility in manipulation of the bunch on each pass through the linac and arcs, and allows for efficient use of space for photon production on each pass.

2.1 Lattice

The lattice of the recirculating accelerator has been designed to permit tunability of the time-of-flight parameters, betatron phase advances, and chromaticity over the different sections of the lattice. For convenience we call the electron beam transport between successive passes of the main linac a "ring". Tracking studies indicate that lattice design is insensitive to errors in magnetic field quality, but needs beam based alignment to correct for alignment errors [15, 25].

Minimizing the footprint of the accelerator imposes a major constraint on global machine parameters such as length and bend radius of the outer (highest energy) transport lines, length of the photon production sections, and the length of the main linac. The circumferences of the arcs of the inner rings are less constrained, although they are carefully selected to allow the machine to be used in a possible future energy recovery mode and with a high electron beam current provided by operation with multiple bunches within the accelerator at any given time. In the case of multi-bunch operation to provide a high average flux, a uniform spacing of all electron bunches in the linac including accelerating and decelerating bunches is highly desirable. The chosen set of ring circumferences provides a wide variety of choices for bunch repetition rate, leading to almost uniform bunch spacing in the 1.3 GHz main linac. Although we do not plan deceleration and energy recovery at this point, the possibility will be available if needed in the future.

The main linac is the simplest part of the machine from a lattice point of view, having no dedicated beam focussing elements. Weak rf focusing is only noticeable on the first pass following injection, when electron beam energies are below few hundred MeV. In all passes after the first the linac acts essentially as a drift space in transverse dynamics — the beta-functions expand quadratically towards both ends of the linac.

A *beam spreader* section transports the electron beam at various energies from the linac into the respective higherenergy rings. Its mirror image a *beam combiner* reconciles different energy orbits from the respective rings into a single line in the main linac. The inevitable proximity of beamlines of different energies results in these sections being rather compact and sophisticated parts of the lattice.

The arc sections transport electrons of a given energy from the end of the beam spreader to the corresponding return straight section for each ring, and back to the beginning of the beam combiner (or to a beam dump in the case of the final "ring"). The magnetic arcs each have a similar lattice, and are comprised of three ~120° betatron phase advance cells each containing a string of bending magnets, three quadrupoles and three sextupoles. The third cell of each arc is used for matching of the arc optical functions to those of the adjoining straight sections. The electron beam transport from the end of the linac to the beginning of straight sections is achromatic and isochronous. However, changes in the time-of-flight parameter (R_{56} matrix coefficient) can easily be provided should electron bunch length adjustment be required at various stages of acceleration (and possibly deceleration). Sextupoles are used to compensate chromaticity and second order terms affecting isochronicity. The dipole bending magnets, quadrupoles and sextupoles in each of the arcs are mechanically identical, allowing cost savings and simplicity.

A tune trombone consisting of four cells, allowing the variation of the betatron tunes over a wide range of approximately ±0.5 with just two parameters, is inserted into each return straight.

The flexibility of the LUX lattice design allows control and preservation of electron beam transverse and longitudinal emittances, minimizing the influence of collective effects. Longitudinal and transverse dynamics have been modeled from the RF gun through the injector linac, the main linac, and the arcs. In the injector, harmonic cavities will be used to control the longitudinal phase-space prior to compression in the arc connecting to the main linac. The bunch length and magnet bend angle in the lowest energy arcs of the machine result in a regime in which coherent synchrotron radiation emission could be expected, and the vacuum chamber geometry is designed to minimize this effect by shielding against lower-frequency radiation. Particle tracking with cavity wakefields, resistive wall impedance, and magnet errors and misalignments, show only modest emittance growth. Coherent synchrotron radiation (CSR) has been studied and reduced aperture in the bend magnets is required to shield against excessive energy spread from this effect [26]. The bunch compressor in the injector arc is specially designed with $-I$ transport lines, where the downstream effects from CSR compensate for CSR induced excitation of the horizontal emittance in the upstream sections [27]. Results indicate that the machine has sufficient flexibility to be able to counteract and balance the effects of CSR and wakefields in the cavities and resistive wall wakefields in the beam transport.

In the harmonic cascade FELs, electrons must be transported between modulator and radiator undulators, while maintaining the charge density modulation in the bunches. A transport line design has been developed in order to maintain the micro-bunching structure at nanometer length scales, requiring all second order aberrations to be corrected.

To reduce remaining aberrations, reversed dipoles are used. With 2 families of trim quads, skew quads and trim sextupoles, respectively, the effect of static errors can be effectively corrected [28]. This lattice also provides for a 5° bend angle, a much simplified design may be possible

with the chosen linear configuration of harmonic cascades.

2.2 Injector systems

The LUX concept requires high brightness electron beams for x-ray production in both FEL's and by spontaneous emission in insertion devices. These requirements are satisfied by a laser-excited, photoemissive electron source, the rf photocathode gun, with the photocathode residing in a high-gradient rf cavity, followed immediately by a short accelerator section to bring the beam up to 10 MeV. Long bunches, of approximately 30 ps, are produced at the cathode to reduce space charge effects and produce low-emittance beams. Following the rf gun a 1.3 GHz superconducting linac accelerates the beam to 200 MeV. The correlated energy spread introduced along the 30 ps bunch by the injector linac is linearized in 3rd harmonic cavities, which prepare the beam for compression in the following arc [27, 29].

Two rf photocathode guns are necessary to produce two classes of beams. Figure 2 shows the injector configuration. The (off-axis) uncoupled or 'round'-beam injector generates low emittance (< 2π mm-mrad) beams used to produce VUV and soft x-rays in the harmonic cascade FELs. The (on-axis) coupled or 'flat'-beam injector produces low emittance (< 3π mm-mrad) beams from a magnetized cathode ($B_z \sim 0.1$-1.0 kG). The angular momentum carried by the 'flat' beam is then used in the downstream adapter optics to create a beam with very small vertical emittance (< 0.3π mm-mrad) and large x/y emittance ratio [30, 31] to produce hard x-rays by spontaneous emission in insertion devices. Both magnetized and unmagnetized beams carry a nominal 1 nC charge within a 30-35ps core. These two beams have separate transport beamlines from the cathodes to the entrance of the linac, and are then merged onto the same beamline for acceleration. Following the injector linac and linearizer cavity, the adapter optics and matching beamlines include pulsed skew and normal quadrupole magnets to produce uncoupled beams with identical beta functions at the entrance to the compressor arc which takes the beam to the main linac. Electron pulses are produced at a rate of 10 kHz in each rf photocathode gun, and bunches from the two high-brightness sources are interleaved.

In order to precisely control the instantaneous current of the electron beam, and thus influence the emittance and energy spread of the electron bunch, temporal modulation must be applied to the laser pulse illuminating the photocathode. Also, the spatial profile of the laser pulse needs to be controlled in order to control the spatial charge distribution of the electron beam, and compensate for non-uniform emission of the cathode surface. Table 1 lists the photocathode laser specifications.

2.2.1 RF photocathode gun design

For production of the "flat" beams, a magnetic field is required at the cathode surface, and a superconducting rf gun is not feasible under these conditions. A copper rf structure is thus employed. The high repetition rate, 10 kHz, of the 30 ps electron beam pulse represents a very low beam duty factor. However, the relatively long filling time of the cavity results in a requirement of approximately 5% rf duty factor, which is much higher than any existing photoinjector and results in a high average power to the cavities. Careful thermal management of the rf photocathode gun is necessary.

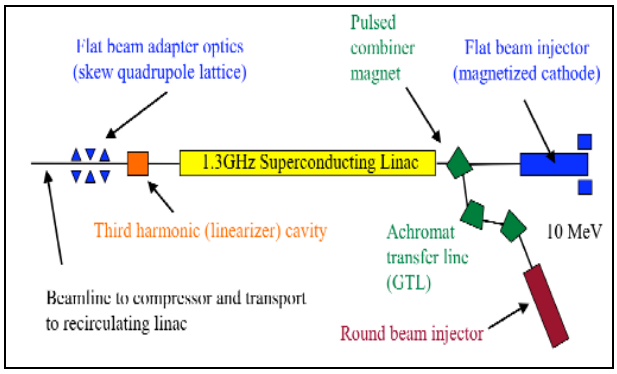

Figure 2. LUX injector layout showing dual rf photocathode guns.

Table 1. Specifications for the photocathode laser.

Wavelength	<270 nm
Pulse energy	1-10 μJ
Pulse width	30-35 ps
Rise/fall time	2-5 ps
Instantaneous power flatness	< 1% RMS
Timing jitter	< 100 fs RMS
Pulse repetition rate	10 kHz
Beam diameter at cathode	2-4 mm
Edge ramp width	0.5 mm
Intensity flatness	< 1% RMS

The design of the cavity, its cooling structure and power couplers, is coordinated with the configuration of the rf system, including a short, high-power driving pulse and active removal of stored energy after the beam pulse to reduce the average power dissipated in the cavity. The design comprises a high-gradient reentrant gun cavity with a photocathode producing a nominal 30 ps bunch with a peak current in the 50 A range. Figure 3 shows the 4-cell rf photocathode gun design [32, 33]. The photocathode is sited on a protruding mesa, facing a reentrant nose-cone that increases the local field on the cathode surface and increases the shunt impedance of the cavity itself. Three identical accelerating cavities increase the beam energy from approximately 2 MeV at the exit of the photocathode cell to 10 MeV. A set of solenoid magnets provides focusing of the beam and emittance compensation [29].

The design of the cavity shape is dictated by requirements of maximizing the shunt impedance to minimize the rf power requirement for high duty factor

operation, distributing the power dissipation over a large area, allowing access for water cooling passages near high power density regions, minimizing multipactoring, as well as optimizing the field profile to provide the required beam emittance. The reentrant structure with curved walls minimizes the peak surface electric fields to 94 MV/m, with 64 MV/m at the photocathode surface. The power dissipated in the cavity walls is 833 kW with 64 MV/m at the photocathode, and an unloaded quality factor Q_u of 19000. The filling time with unity coupling is 2.34 μs, and a 5 μs pulse will fill the cavity to 88% of maximum gradient, so the rf drive power must be raised to 1075 kW to bring the cavity to desired gradient at the end of 5 microseconds. At a 10 kHz repetition rate, the total power dissipated in the cavity is 31.3 kW, with peak wall power densities up to 98 W/cm^2.

Three techniques have been studied to reduce the cavity wall power density [33]:

- Reduce the rf drive pulse duration and increase the peak power
- Increase the coupling ß to the rf source to reduce the filling time
- Actively remove the stored energy in the cavity

Each of these techniques will increase the peak power required of the klystron and the power dissipated in the dummy load of the circulator between the klystron and the cavity, but the reduction in cavity power is significant. Actively removing the power from the cavities by reversing the drive phase of the rf power will remove the stored energy over approximately 2 μs and deposit it in the dummy load associated with the circulator.

If the stored energy is actively removed from the cavity as described above, the total thermal power may be reduced to only 67% of the equivalent square wave rf pulse in the cavities. The reduction in wall power density is significant, with the peak wall power density in the first cell decreasing from 98 W/cm^2 for the square-wave case to 66 W/cm^2 with active stored energy removal. The photoinjector design incorporates water-cooling passages integral to the cavities themselves.

A finite element analysis has been carried out to characterize the electromagnetic, thermal and structural behavior of the photoinjector cavity subject to the prescribed rf power loading. A single ANSYS [34] model has been developed to perform all of the calculations using a multi-step process [33, 35]. The model is constructed to take advantage of the four-fold symmetry of the cavity about the beam axis. The rf solution is obtained as a modal analysis of the cavity, and the surface element results are available in the form of E and H field data. The H field at each surface node is used to calculate the resulting heat flux based on the surface resistance, the element areas, and a scale factor derived from the expected total average power loss in the cavity of 31 kW. A new identical surface mesh with the appropriate thermal elements is generated, and the heat flux loads are automatically transferred to the thermal model. Heat balance is achieved in the model by applying convective cooling to the surfaces of the water passages.

The cavity model and the resulting temperature contours for 20°C cooling water are shown in Figure 4, with a maximum temperature rise of approximately 70° C. ANSYS allows direct solution of the structural problem by means of converting the thermal elements to their equivalent structural elements. The temperature data obtained from the thermal solution is applied as a load on the structural model. Vacuum loads, symmetry boundary conditions and cavity support constraints are applied as well. The peak von Mises stress in the photoinjector was found to be approximately 65 MPa.

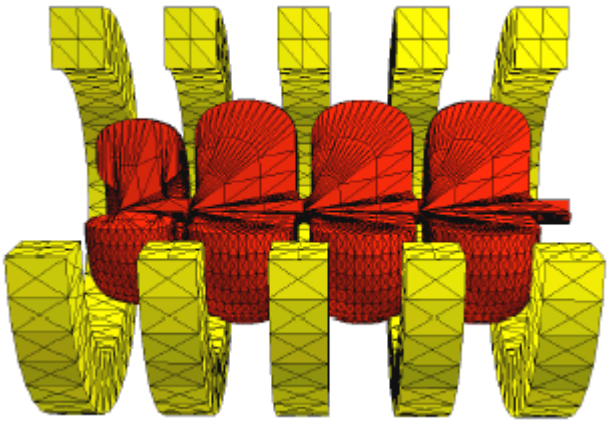

Figure 3. CAD model of the rf photocathode gun, showing cathode cell, three accelerating cells, and focusing solenoids. The cathode is mounted on a conical protrusion on the axis of the cavity at left, the electron beam exits the beampipe to the right of the figure. The laser pulse enters the cavity from the beampipe to illuminate the cathode.

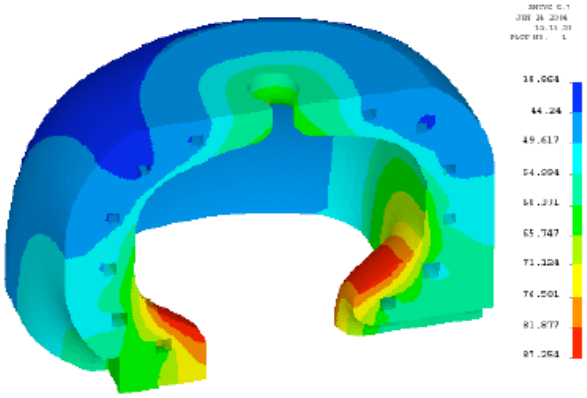

Figure 4. Steady-state ANSYS model of the cathode cell, showing temperature contours.

2.3 Superconducting linac and cryogenics

Superconducting rf structures have advantages in providing extremely stable rf fields, and inherently small perturbative effects on the beam. Taking advantage of advances made in superconducting rf technology in recent years, the parameters of the proven TESLA

superconducting rf systems have been used in LUX design studies for the linacs[36].

The large quality factor of superconducting structures ($Q_0 \sim 10^{10}$) results in a long filling time of 2.4 s for unloaded 1.3 GHz structures. Overcoupling the cavity to the rf power input port reduces the quality factor, but requires additional rf power to overcome reflections at the coupler. The beam loading from a 10 μA injected beam is small, and significant overcoupling has a direct consequence in increased rf power costs. Thus the coupling, the loaded quality factor Q_l, and the filling time are limited primarily by the ability to provide feedback of the system against field fluctuations induced by microphonics [15, 36]. A 50 Hz bandwidth is selected in order to provide adequate feedback response, resulting in an external quality factor Q_e of 2.6×10^7, and the cavity filling time is then several tens of microseconds. Typically, power is applied to standing wave cavities for about three time constants before the beam enters the structure, to allow time for energy to build up in the cavity so that the required field can be developed. Since we want to operate at bunch rates of 10 kHz, the required repetition time of 100 s is too short to change the field in the cavities commensurately, and the superconducting linac must be operated in continuous wave (cw) mode. The resultant power dissipation due to rf currents on the cavity inner surfaces increases significantly over the TESLA design parameters,.

The main linac is required to provide 1 GeV energy gain per pass, and the design uses six cryomodules each containing nine cavities. The cavity gradient required is then 18.5 MV/m, and we specify 20 MV/m to provide margin in accommodating operating off-crest, some rf systems off-line, and poor performance of some cavities. Operating in cw mode at a gradient of up to 20 MV/m requires development of cryogenic systems to accommodate the thermal load. A nine cell cavity operating in cw mode at 20 MV/m will generate 42 W heat load as a result of rf current flow on the inner surfaces of the cavity [15]. Added to this is 8.5 W heat entering the cavity niobium body from the input rf power coupler. This dynamic heat load is to be transferred through the niobium to the cavity outer surface in the super-fluid helium liquid bath, then to the super-fluid helium surface where boiling occurs at 1.8 K, without quenching the cavity. In a super-fluid helium test bath there is no problem transferring this heat from the cavity outer surface to the super-fluid helium surface, however, the transport of about 50 W from the cavity outer surface through the helium tank, the feedpipe and the header-pipe configuration proposed for the TESLA cryomodules will require some modifications.

In order to provide sufficient heat transfer from the cavity outer surface to the surface of the liquid in the header, the following modifications to the basic TESLA cryogenic module design are under consideration:

- The number of feed pipes between the rf cavity helium tank and the two-phase helium stand pipe may be increased from one to two
- The helium feeds may enter the helium tank near the ends so heat can flow two ways along the rf cavity. If one puts the feeds at the one-quarter and three-quarter points along the cavity, the flow along the cavity is split fourways, and cavity cool down is not as effective
- The inside diameter of the helium tank may be increased by 10 to 15 mm to increase the spacing between the cavity convolutions and the cavity helium tank inner wall
- The liquid helium feed pipes from the stand-pipe to the tank may have their inside diameter increased from 60 mm to 100 mm
- The two-phase helium header pipe may have its inside diameter increased from 70 mm to 100 mm to allow heat to flow through the liquid in a half full pipe

In addition to the linacs, superconducting rf structures are required for the deflecting cavities (see Section 3), and for the linearizing 3rd harmonic cavities (Section 2.2). A seven-cell 3.9 GHz cavity has been designed as a deflecting structure. Operating in the first dipole-mode, the cavity is phased such that the beam centroid passes at the zero-crossing of the field, and the bunches receive opposite transverse kicks to the head and tail. Design details are given in [15, 37].

2.4 Collective effects

The performance of LUX depends on preservation of transverse emittances and energy spread through the linac and the arcs. The flexibility of the LUX lattice design allows control and preservation of electron beam transverse and longitudinal emittances, minimizing the influence of collective effects, as discussed in section 2.1 above. Longitudinal and transverse dynamics have been modelled from the rf gun through the injector, the main linac, and arc sections. The bunch length and magnet bend angle in the lowest energy arcs of the machine result in a regime in which coherent synchrotron radiation emission could be expected, and the vacuum chamber geometry is designed to minimize this effect by shielding against lower-frequency radiation [26]. CSR effects predominantly influence the head and tail of the bunch, leaving the core relatively unaffected [26, 38].

The short-range transverse wake fields from the linac cavities are a potential source of emittance growth, and the size of the transverse kick from the wake fields increases with increasing offset of the bunch from the axis of the cavity, so there are possible implications for the alignment of the cavities and orbit control. Resistive wall wakefields may be particularly strong in the narrow-gap insertion devices. Investigations including the nominal bunch distribution and tracking through various sections of the machine show that one must always pay attention to these aspects in the design phase, however they do not present insurmountable problems towards obtaining the machine design parameters [15, 38].

The influence of long-range wake fields on the emittance growth is also expected to be a minor effect [38].

2.5 Other systems

The vacuum systems design for a single-pass system is less demanding than typical third-generation synchrotron light sources, as a result of the reduced average beam current and outgassing from synchrotron radiation heat load on vacuum surfaces, and modest beam lifetime requirements. A system with a large manifold cryogenically pumped and periodically attached to the beampipe has been designed as a low-cost option [39].

Lattice magnets are of conventional water-cooled electromagnet design, based on those of the Advanced Light Source (ALS) booster quadrupoles and sextupoles. Magnets in each of the arcs are mechanically identical, allowing cost savings and simplicity [15].

Radiofrequency power systems have been designed to provide 20 MV/m accelerating gradient in cw mode, with 50 Hz bandwidth to control cavity resonance perturbations due to microphonics [15].

A beam dump has been designed to accommodate up to 100 kW beam power, allowing for significant increase in bunch current or repetition rate. Conventional facility requirements are similar to those for existing third generation synchrotron light sources, with stable foundations and thermal control of the accelerator enclosures.

3. PHOTON PRODUCTION AND X-RAY BEAMLINES

LUX is designed as a source to produce high-flux x-ray pulses with duration of 100 fs or less at a 10 kHz repetition rate, optimized for the study of ultra-fast dynamics. To provide a range of photon wavelengths facilitating spectroscopies and diffraction, two techniques are employed for photon production. Cascaded harmonic generation in FELs produces coherent radiation in the VUV-soft x-ray regime, and a specialized technique is used to compress spontaneous emission for ultra-short-pulse photon production in the 1-10 keV range. The facility design provides independently tunable x-rays at each beamline endstation, and up to approximately 20 endstations.

The uncoupled beam with nearly equal x,y emittances is used in the cascaded harmonic generation scheme, where the FEL process is initiated by a coincident seed laser pulse. The process is similar to that of high-gain harmonic generation (HGHG) demonstrated at the DUV FEL [21, 40, 41]. One, two, and three-stage harmonic cascade FELs are shown in the return straights in Figure 1. After the final pass through the main linac, the 3 GeV beam is switched between four-stage harmonic cascades to generate nm-wavelength x-rays, and the hard x-ray photon production section.

We have developed a technique for production of attosecond duration x-ray pulses using an optical laser to selectively excite a controlled short section of the electron beam into resonance in the harmonic cascade FEL [14]. Accessing the sub-femtosecond time domain opens new possibilities in experimentally determining dynamics on the timescales of electronic transitions in atoms.

In the proposed VUV-soft x-ray production scheme, a laser-seeded harmonic-cascade FEL produces high-flux, spatially and temporally coherent, nearly transform-limited, short-pulse photons over an energy range of tens of eV to ~1 keV [19, 20]. In this process the uncoupled (nearly equal x,y emittance of 2 mm-mrad) high-brightness electron beam of 500 A peak current, ± 200 keV energy spread, is passed through an undulator where a co-propagating seed laser modulates the charge distribution over a short length of the bunch, typically 10-100 fs duration. The imposed modulation results in enhanced microbunching and eventual coherent radiation at both the fundamental and harmonics of the seed modulation wavelength. In a following FEL the beam radiates at a selected shorter wavelength, in an undulator tuned to a harmonic of the seed laser. The electron bunch is then delayed in a short chicane, and the process repeated by modulating a fresh portion of the beam this time with the harmonic radiation produced in the previous undulator. Using an optical parametric amplifier as the seed with wavelength 200-250 nm, and variable undulators in each harmonic cascade FEL, allows significant tunability in up to four stages of harmonic generation. Output power levels in the VUV to soft x-ray wavelengths are in the range 10-100's MW from a 100 MW seed laser and undulator lengths typically a few to several meters. With the LUX parameters, coherent x-rays with wavelength as short as 1 nm are achievable at 3 GeV. Wavelength tuning and pulse duration are determined by laser parameters and undulator K-values. We note that development of suitable VUV-soft x-ray lasers by high-harmonic generation (HHG) in gases would allow seeding at shorter wavelelengths, potentially reducing the number of harmonic cascade stages required. Circular polarization of the x-ray beam may be attainable by use of elliptical undulators, and flux stability of 0.1% or better is obtained in seconds from random pulse-pulse flux variations of 10-20% at 10 kHz repetition-rate.

Hard x-rays are produced by the 3 GeV electron beam in an array of narrow-gap short-period insertion devices indicated in Figure 1. At the exit of the final arc the 'flat'-beam electron bunches receive a time-correlated vertical kick in a dipole-mode rf cavity. This imparts to the electron bunch a transverse momentum that is correlated in amplitude to longitudinal position within the bunch. The electrons then radiate x-rays in the downstream chain of undulators and dipole magnets, imprinting this correlation in the geometrical distribution of the x-ray pulse. The correlated x-ray pulse is then compressed by use of asymmetrically cut crystal optics to achieve the ultra-short x-ray pulse length [15, 16, 22]. Narrow-gap in-vacuo superconducting undulator designs provide tunable x-ray sources in the 1–12 keV range. Wigglers may also be used to provide a broad x-ray spectrum.

There are several qualitative differences between LUX and electron storage ring requirements for hard x-ray optics and beamlines. Firstly, the hard x-ray beamlines must accommodate the position or angle correlation of the electron bunch - in the wigglers, electrons will have a vertical *position*-time correlation, in the undulators, a vertical *angle*-time correlation [15, 16, 22, 42]. Secondly, the average current is low, 10 μA, and consequently, the total power radiated by the undulators and wigglers is also low, typically 0.4 W. None of the high power optical engineering typical of the third generation synchrotron radiation sources is required, and silicon or fused silica optics can be used without water cooling. The design of the photon stops in the front ends is also simplified.

Narrow-gap in-vacuo superconducting undulator designs provide tunable high-flux sources of spontaneous emission hard x-rays. A typical undulator will have 2 m length, 1.5 cm period, 4 mm gap and 2 T peak field on axis, resulting in an optimal photon energy range of 1.4 to 12 keV at 3 GeV beam energy. The spectral shape of the undulator harmonics is modified by the angular correlation of the electron bunches, and the undulator beamline vertical acceptance is increased from 50 to 500 μrad in order to accept the larger angular divergence of the beam. The angular correlation broadens the undulator harmonic, but the peak flux is unchanged. This result can be understood from the fact that each electron is radiating essentially the same spectrum but with a variation of the on-axis direction. The brightness is, however, decreased by the increase in the angular divergence.

Wigglers provide intense hard x-ray sources with a continuous spectrum extending to high photon energy. However, because wigglers produce incoherent radiation, the depth of source effect must be considered. The hard x-ray pulse compression scheme depends on the small vertical source size. The effective source is calculated by projecting the radiation from along the length of the wiggler onto a vertical plane at the center and then convoluting with the electron beam. Considering the case of a 60 cm long wiggler and 0.2 mrad vertical acceptance, the effective source size is 33 μm (fwhm) compared with 26 μm (fwhm) for the electron beam. Consequently, wigglers can be used at LUX consistent with the x-ray pulse compression scheme.

Asymmetrically cut crystals may be used as optical elements in a hard x-ray pulse compression scheme. As a result of the different angles of incidence and diffraction, a crystal may be oriented to produce a variable path length across the xray beam. When the variation in the optical path length matches the spatial correlation of the incident x-rays an ultrafast x-ray pulse is produced. Two crystals are used in order to provide a fixed exit beam direction while changing the photon energy.

X-ray beamline optics for the coherent VUV and soft x-ray beams produced in the FEL's must accommodate a high peak intensity ~ 0.06 J/cm^2, and average powers similar to those of existing 3rd generation light sources. The position of the first mirrors should be 10 m from the center of the radiator insertion device. A beamline configuration aperture - horizontal mirror - vertical mirror – endstation provides the full 10^{-4} bandwidth of the FEL (no grating). An aperture - vertical mirror – grating – slit – grating – vertical mirror - horizontal mirror – endstation beamline configuration provides a bandwidth of 90 meV at 280 eV (C K edge), in a length of 13.3m.

4. LASERS AND SYNCHRONIZATION

Sophisticated laser systems will be an integral part of the LUX facility, providing experiment excitation pulses, and stable timing signals, as well as the electron source through the photocathode laser. Each endstation will have it's own dedicated laser system and optical manipulation and diagnostics, and optical tables and equipment will be contained within a stable and controlled environment. Multiple tuneable lasers covering a range of approximately 200-3000 nm and pulse durations of ≤ 50 fs are required for experiment initiation, together with temporal and spatial filtering to optimize performance for specific experimental applications.

X-ray pulses are synchronized to pump lasers for pump-probe experiments by a timing system based on a modelocked laser distributing optical pulses over stabilized fiber optic lines [15, 23, 24]. Distribution systems using fiberoptic transmission lines will provide optical seed pulses from the laser master oscillator to multiple remote locations throughout the facility, with path lengths stabilized by feedback based on optical interferometric measurements. Generating microwave signals from the optical pulse train then allows for locking of the beamline endstation lasers to this common master oscillator. Each laser then has flexibility in amplitude, wavelength, and delay, while timing jitter with respect to the master oscillator is reduced to ~ 10's femtoseconds. Accelerator rf signals are also derived from the laser master oscillator, and feedback around the rf systems maintains their lock to the master oscillator.

Synchronization of the ultra-short x-ray pulses to the experimental excitation pulse is critical to studies of ultra-fast dynamics. In the LUX facility concept timing jitter is inherently reduced by photon production techniques of seeded FEL systems, and bunch manipulation followed by x-ray compression. In the case of EUV and soft x-ray production, the cascaded harmonic generation seed laser oscillator also drives the sample excitation laser, resulting in timing stability of approximately 20 fs. For our scheme of hard x-ray production by bunch manipulation followed by x-ray pulse compression, we find that the phase jitter of the deflecting cavities with respect to the experimental laser pulse dominates timing issues [15, 23]. Phase and amplitude feedback of the deflecting cavities is expected to provide x-ray pulse to laser pulse timing stability of 50 fs or better.

SUMMARY

LUX is a recirculating linac-based facility concept designed to address the growing need for ultrafast x-ray scientific research. The facility is specifically designed

with a view toward solving problems in ultrafast science, with integrated laser systems, multiple independently tunable x-ray beamlines covering a wide spectrum, and tight synchronization between laser pump and x-ray probe beams. Access to dynamics in the sub-femtosecond time-domain is envisioned with FEL x-ray radiation with application of a special technique using modulation of electrons using a short-pulse laser.

ACKNOWLEDGEMENTS

This work was supported by the U.S. Department of energy under Contract No. DE-AC03-76SF00098

REFERENCES

1. 2004 workshop on "Ultrafast X-ray Science", April 28-May 1, La Jolla Marriott, San Diego, CA, http://ultrafast2004.lbl.gov/
2. Workshop on "Attosecond Physics", The Institute for Theoretical Atomic, Molecular and Optical Physics (ITAMP), November 20-22, 2003, Harvard University, http://itamp.harvard.edu/workshops.html
3. Summer School on "Ultrafast X-Ray Science", July 13-19 2003, Cargese, Corsica, France, http://wwwy.ensta.fr/ufx/
4. Workshop on "Ultrafast Science with X-rays and Electrons", 9-12 April 2003, Montreux, Switzerland, http://sls.web.psi.ch/view.php/science/events/uscience03/index.html
5. Workshop on "Ultrafast Phenomena by Synchrotron Radiation", October 28-29, 2002, I.C.T.P. - Strada Costiera, 11,Trieste, Italy, http://www.elettra.trieste.it/events/conferences/um_x/ultra-program.html
6. Workshop on "New Opportunities in Ultrafast Science using X-rays", April 14-17 2002, Napa, CA http://wwwesg.lbl.gov/esg/meetings/ultrafast/
7. Cavalleri et al. *Phys. Rev. Lett.* 87, 237401 (2001)
8. Schotte, et al, Science 300, 1944 (2003)
9. Glandorf, et al, Phys. Rev. Lett. 87, 193002 (2001)
10. M. Hentschel et al., Nature, v.414, p. 509 (2001)
11. The Linac Coherent Light Source, http://www-srl.slac.stanford.edu/lcls/
12. The TESLA Test Facility, http://tesla.desy.de/new_pages/0000_TESLA_Project.html
13. The European X-Ray Laser Project, XFEL, http://xfel.desy.de/content/e169/index_eng.html
14. A. Zholents, W. Fawley, "Proposal for Intense Attosecond Radiation from an X-Ray Free-Electron Laser", Phys.Rev. Lett. **92**, 224801 (2004)
15. J. N. Corlett et al, "Feasibility study for a recirculating linac-based facility for femtosecond dynamics", LBNL formal report LBNL-51766, December 2002.
16. J. N. Corlett et al, "A Recirculating Linac Based Synchrotron Light Source for Ultrafast X-ray Science", Proc. EPAC2002, Paris, June 2002.
17. J. N. Corlett et al, "A Recirculating Linac-Based Facility for Ultrafast X-ray Science", Proc. 2003 Particle Accelerator Conference (IEEE, 2003).
18. J.N. Corlett et al, "LUX - A Recirculating Linac-based Ultrafast X-ray Source", Synchrotron Radiation & Instrumentation SRI03, San Francisco, August 2003. LBNL-53617.
19. W. Fawley et al, "Simulation studies of an XUV/soft x-ray harmonic-cascade FEL for the proposed LBNL recirculating linac", Proc. 2003 Particle Accelerator Conference, Portland, Oregon, May 12 - 16, 2003, May 2003.
20. G. Penn et al, "Harmonic Cascade FEL Designs for LUX", Proc. EPAC2004, Lucerne, July 2004.
21. L.-H. Yu et al, "High-Gain Harmonic-Generation Free-Electron Laser", Science **289** 932-934 (2000).
22. A. Zholents et al "Generation of subpicosecond x-ray pulses using RF orbit deflection", NIM A 425 (1999) 385-389.
23. J.N. Corlett et al, "Techniques for Synchronization of X-ray Pulses to the Pump Laser in a Ultrafast X-ray Facility", Proc. 2003 Particle Accelerator Conference, Portland, Oregon, May 12 - 16, 2003, LBNL-52607, May 2003.
24. R. B. Wilcox, J. W. Staples and L. R. Doolittle, "A fiber optic synchronization system for LUX", Proc. EPAC2004, Lucerne, July 2004.
25. A. Zholents et al, "Initial Lattice Studies for the Berkeley Femtosecond X-ray Light Source", Proc. EPAC2002, Paris, June 2002.
26. A. Zholents, "Longitudinal phase space control in the Berkeley femtosecond x-ray light source LUX", Proc. 2003 Particle Accelerator Conference, Portland, Oregon, May 12 - 16, 2003, May 2003.
27. S. Lidia, et al, "An Injector for the Proposed Berkeley Ultrafast X-Ray Light Source", Proc. 2003 Particle Accelerator Conference, Portland, Oregon, May 12 - 16, 2003, May 2003.
28. W. Wan et al, "Design Study of the Bending Sections between Harmonic Cascade FEL Stages", Proc. EPAC2004, Lucerne, July 2004.
29. S. M. Lidia, "Design of Injector Systems for LUX", Proc. EPAC2004, Lucerne, July 2004.
30. R. Brinkmann, Y. Derbenev, K. Flottmann, "A low emittance, flat-beam electron source for linear colliders", Phys. Rev. STAB, Vol. 4, 053501 (2001).
31. D. Edwards et al, "The Flat Beam Experiment at the FNAL Photoinjector", Proc. XXth International Linac Conference, Monterey, 2000.
32. J. Staples et al, "The LBNL femtosource (LUX) 10 kHz photoinjector", Proc. 2003 Particle Accelerator Conference, Portland, Oregon, May 12 - 16, 2003, May 2003.
33. J. Staples, S. Virostek, S. Lidia, "Engineering design of the LUX photoinjector", Proc. EPAC2004, Lucerne, July 2004.
34. ANSYS is a registered trademark of SAS IP, Inc.
35. N. Hartman and R.A. Rimmer, "Electromagnetic, Thermal, and Structural Analysis of RF Cavities

using ANSYS", Proc. 2001 Particle Accelerator Conference, IEEE.
36. TESLA Technical Design Report, DESY 2001-011, March 2001.
37. D. Li and J. N. Corlett, "Deflecting rf cavity design for a recirculating linac-based facility for ultrafast x-ray science (LUX)", Proc. 2003 Particle Accelerator Conference, Portland, Oregon, May 12 - 16, 2003, May 2003.
38. J. Corlett et al, "Collective effects analysis for the Berkeley femtosource", Proc. 2003 Particle Accelerator Conference, Portland, Oregon, May 12 - 16, 2003, May 2003.
39. R.P. Wells, J.N. Corlett, and A. Zholents, "Re-Circulating Linac Vacuum System", Proc. 2003 Particle Accelerator Conference, Portland, Oregon, May 12 - 16, 2003, LBNL-52623, May 2003.
40. L.-H. Yu et al, "First ultraviolet high-gain harmonic-generation free-electron laser", Phys. Rev. Let. Vol 91, No. 7 (2003)
41. A. Doyuran, L. DiMauro, W. Graves et al, Phys. Rev. ST Accel. Beams 7, 050701 (2004)
42. P.A. Heimann, H.A. Padmore and A.A. Zholents, "X-ray optical designs for the Linac-based Ultrafast X-ray source (LUX)," SPIE Proceedings 5194, 39 (2004).